International Journal of Nanomedicine

Dovepress
open access to scientific and medical research

Open Access Full Text Article

ORIGINAL RESEARCH

ROS-Generating Poly(Ethylene Glycol)-Conjugated Fe_3O_4 Nanoparticles as Cancer-Targeting Sustained Release Carrier of Doxorubicin

Boddu Adilakshmi[1], Obireddy Sreekanth Reddy[2–4], Duddekunta Hemalatha[1], Kummari SV Krishna Rao[1], Wing-Fu Lai[2,3]

[1]Polymer Biomaterial Design and Synthesis Laboratory, Department of Chemistry, Yogi Vemana University, Kadapa, Andhra Pradesh, 516005, India; [2]Department of Urology, Zhejiang Provincial People's Hospital, Hangzhou Medical College, Zhejiang, 310012, People's Republic of China; [3]Department of Applied Biology and Chemical Technology, Hong Kong Polytechnic University, Hong Kong Special Administrative Region, People's Republic of China; [4]Department of Chemistry, Sri Krishnadevaraya University, Anantapuramu, Andhra Pradesh, 515003, India

Correspondence: Wing-Fu Lai; Kummari SV Krishna Rao, Email rori0610@graduate.hku.hk; ksvkr@yogivemanauniversity.ac.in

Purpose: Site-specific drug delivery systems can contribute to the development and execution of effective cancer treatment. Due to its favorable features (including high biocompatibility, high hydrophilicity and ease of functionalization), poly(ethylene glycol) (PEG) has been widely adopted to design drug carriers. Generating carriers for delivery of hydrophobic anticancer agents, however, is still a challenge in carrier design.

Methods: In the first step, PEG is functionalized with dialdehyde to generate PEG-$(CHO)_2$ using EDC/NHS chemistry. In the second step, Fe_3O_4 nanoparticles are functionalized with amino groups to generate Fe_3O_4-NH_2. In the third step, PEG-$(CHO)_2$, Fe_3O_4-NH_2 and doxorubicin (DOX) react in an acidic environment to yield a drug conjugate (PEGDA-MN-DOX), which is subsequently characterized by FT-IR, ^{1}H-NMR, SEM, TEM, DLS, TGA, and DSC.

Results: The chemical functionalities of the drug conjugate are confirmed by FTIR, H-NMRand XRD analysis.The release pattern of PEGDA-MN-DOX is investigated at 25 and 37 °C at different pH values. The results indicate that the developed drug conjugate cannot only behave as a sustained-release carrier, but can also generate a significant level of reactive oxygen species (ROS), leading to a high level of toxicity against MCF-7 cells while still showing excellent biocompatibility in 3T3 cells.

Conclusion: The reported conjugate shows anticancer potential, cancer-targeting ability, and ROS-generating capacity for effective drug encapsulation and sustained release in chemotherapy.

Keywords: PEG, doxorubicin, magnetic nanoparticles, anti-cancer, biocompatibility, drug delivery

Introduction

Cancer is a group of diseases characterized by abnormal cell proliferation. According to a recent global projection, the number of cancer sufferers will exceed 15 million by 2020,[1] with 13.1 million people being killed by the disease by 2030.[2] Doxorubicin is an anthracycline drug that has been widely used in cancer treatment. Despite its broad-spectrum anticancer activity, its clinical use has been limited by its adverse effects, particularly cardiotoxicity. This is especially true for patients with advanced illnesses who need a high dose. This problem, however, has been ameliorated by recent advances in nanotechnology. A good example is the emergence of liposomal doxorubicin hydrochloride injection, which is the first clinically approved liposomal formulation to work against solid tumors, transplantable leukemias, and lymphomas.[3] Another example is magnetite nanoparticles (MNs) and other magnetic nanoparticles with high saturation magnetization and magnetic susceptibility. These nanoparticles have attracted research interest because the magnetic characteristics enable applications in medical diagnosis and treatment, ranging from immunoassay and magnetic resonance imaging to hyperthermia.[4–6] All these demonstrate the promising potential of nanomaterials in biomedical applications.[4–10]

Received: 19 June 2022
Accepted: 7 September 2022
Published: 21 October 2022

Graphical Abstarct

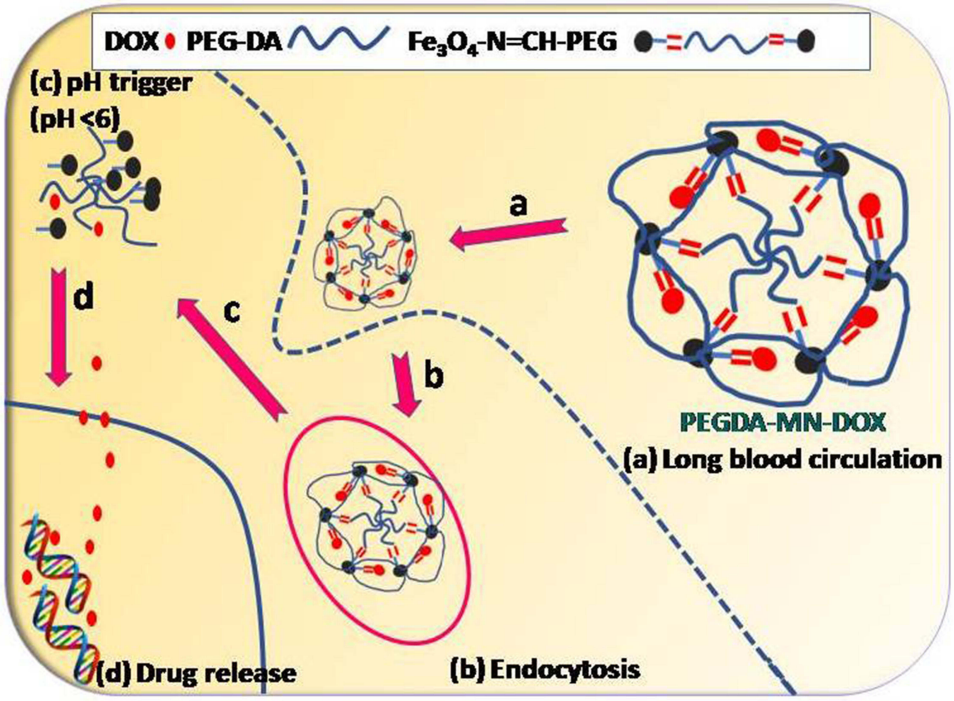

As far as drug delivery using nanocarriers is concerned, one of the most significant biological barriers to be tackled is opsonization. Opsonin is a protein found in blood serum. It can bind to conventional non-stealth nanoparticles, allowing mononuclear phagocytic system (MPS) macrophages to recognize and eliminate these nanoparticles before they can perform their intended therapeutic function. A few methods for masking or camouflaging nanoparticles have been developed. Poly(ethylene glycol) (PEG) conjugation to the surface of nanoparticles is one of these methods. The addition of PEG and PEG-containing copolymers to the nanoparticle surface significantly increases the blood circulation half-life of the nanoparticles. This technique creates a hydrophilic barrier around the nanocarrier, which, due to steric repulsion forces, blocks and delays the onset of opsonization. In fact, besides using PEG, surface modification by other chemicals such as amino silanes, chitosan, and carbodiimide have been reported to coat and functionalize the nanoparticle surface.[6] In an earlier study, Ali Dabbagh and coworkers have coated MNs with PEG and have exploited the porous nature of the generated nanoparticles for DOX encapsulation and controlled release.[7] Recently, different thermosensitive agents have also been used to coat the surface of MNs to prevent uncontrolled leakage of encapsulated pharmaceuticals.[7,8]

The fact that most chemotherapeutic techniques for cancer treatment are nonspecific is a significant disadvantage. Intravenous administration of chemotherapeutic agents (usually cytotoxic) results in systemic toxicity because the agents kill both normal cells and tumor cells.[9] Use of a drug carrier which has undergone surface functionalization to enhance targeting specificity and controlled drug release is desirable. The later can be achieved by using covalent and non-covalent strategies for carrier modification.[11–15] Among all, PEG has been commonly used because not only of its hydrophilicity and biodegradability but also its ability to prolong the circulation time of the drugs in blood,[16,17] resulting in high drug accumulation at tumours through enhanced permeability and retention (EPR) effects.[18,19] By considering the above facts, in this study, MNs are chemically conjugated with PEG along with DOX. The designed systems provide several features ie, EPR effect, high drug loading, triggered release of the drug, and ROS-generating capacity.

Experimental

Materials

PEG (Mw = 6000 Da), ferrous chloride tetrahydrate, ferric chloride hexahydrate, and ethylene diamines were obtained from sigma Aldrich (St. Louis, MO, USA). Sodium hydroxide, isopropanol, methanol, ethanol, glacial acetic acid, and monochloroacetic acid were purchased from SD fine chemicals Ltd. (Mumbai, India). Doxorubicin hydrochloride (DOX) was obtained from Aspire Pharma (Telangana, India). All other reagents were used as received. Double distilled water was used throughout the experiments.

Preparation of PEG-Dialdehyde

PEG-dialdehyde was synthesized according to the procedures previously reported.[17] In brief, PEG (0.64 mmol) was solubilized in 100 mL of dry dichloromethane. A required amount of 4-carboxybenzaldehyde (0.22 g, 1.46 mmol) was then added. The mixture was allowed to cool to 5°C. To this reaction mixture, DCC (0.41 g, 2 mmol) and DMAP (0.24 g, 0.2 mmol) were added. The reaction was conducted for 24 h at 40°C. After that, the reaction mixture was filtered to remove dicyclohexylurea. The product was concentrated using a rotary evaporator and precipitated in diethyl ether. It was dried in an oven at 40 °C (yield = 91.4%).

Preparation of Functionalized MNs

MNs were synthesized by a co-precipitation technique using ferrous and ferric salts. In brief, 3.2 g of $FeCl_3.6H_2O$ and 1.2 g of $FeCl_2.4H_2O$ were dissolved in 200 mL of deoxygenated distilled water and stirred at 300 rpm for 1 h under a nitrogen atmosphere. To this reaction mixture, 20 mL of ammonium hydroxide (30%) and 40 mL of ethylene diamine were added slowly and stirred at 60°C for 1 h to form aminated MNs (aminated-MNs). The black precipitate was collected by magnetic separation and washed with distilled water, dried in the air, and finally stored in airtight containers for further use.[14]

Preparation of DOX-Loaded PEG-Dialdehyde-MNs (PEGDA-MN-DOX)

MNs were dispersed in 50 mL of dry methanol and sonicated for 30 min. PEG-dialdehyde (PEGDA) (0.2 g) and DOX (0.02 g) were added to the above solution. To this mixture, a catalytic amount of acetic acid was added and stirred vigorously for 12 h. The solvent was removed under reduced pressure to obtain a dark brown product. The product was purified twice with anhydrous diethyl ether. The same procedure was used to prepare drug-free PEGDA-MNs but no DOX was added during the process.

In vitro Drug Release Studies

In vitro release studies of DOX from PEGDA-MN-DOX were carried out at pH 7.4 and 1.2 at 37°C. In order to estimate the release of DOX from PEGDA-MN-DOX, 15 mg of dried nanoparticles were taken in different pH solutions in a dissolution tester (LABINDIA, DS-8000, India) at predetermined intervals. The dialysate was taken from each basket and refilled with an equal volume of fresh buffer solution. Drug release profiles were determined by using UV-Vis spectrophotometry (LABINDIA, UV-Vis 3092, India) at 490 nm.

Cytotoxic and Reactive Oxygen Species (ROS) Studies

The ability of DOX, PEGDA-MN, and PEGDA-MN-DOX to kill MCF-7cells [purchased from the American Type Culture Collection (ATCC; Manassas, VA, USA)] was studied by performing an MTT assay, in which cell-seeded 96-well plates were incubated in an atmosphere of 5% CO_2 for 24 h. After incubation, samples were introduced into each well plate to determine the viability of the cells. 10 µL of the MTT solution (5mg/mL) was applied to each well, which was incubated for another 4 h. The supernatant was removed and refilled with 100 µL of DMSO in each well. The absorbance was measured at 540 nm using a UV-Vis spectrophotometer. The IC_{50} value was determined using the linear regression equation ($y = mx+c$), with the value of y being taken as 50. The values of m and c were derived from the cell viability data. The ROS-generating capacity of a sample was analyzed using 2.7-dichlorodihydrofluorescein diacetate (H_2DCFDA) as described in an earlier study.[20]

Structural Characterization

The structure of PEGDA was characterized by using proton nuclear magnetic resonance (^{1}H-NMR) spectroscopy (400 MHz) (Bruker Avance III; Bruker, USA), Fourier-transform infrared (FTIR) spectroscopy (Bomem MB-3000; ABB Corporate, Zurich, Switzerland) spectra of pure DOX, PEG-dialdehyde, PEGDA-MN, and PEGDA-MN-DOX nanoparticles were collected in the range of 400- 4000cm^{-1}. Thermogravimetric analysis (TGA) and differential scanning calorimetry (DSC) curves of the samples were recorded using TA instruments (STA, Q600, USA), with the samples being heated at a scan rate of 10°C/min in the presence of an inert atmosphere. X-ray diffraction (XRD) patterns of the samples were analyzed using an X-ray diffractometer (Rigaku, Mini flex 600, JAPAN) using Cu αK radiation (scan speed of 10°/min). The surface morphology of the samples was analyzed by using scanning electron microscopy (SEM) (JOEL, IT500A, Japan). Using transmission electron microscopy (TEM)(JEOL JEM 2100; JEOL, Japan) and dynamic light scattering (Zetasizer ver. 7.10, Malvern Instruments Ltd., UK) instruments, the sizes of the amine-functionalized MNs and PEGDA-MN-DOX nanoparticles were measured.

Results and Discussion

Characterization

The nuclear magnetic resonance (^{1}H-NMR) spectrum of PEGDA (Figure 1) shows peaks at 10.10 ppm (Ar-CHO), 8.18 ppm (aromatic protons), 7.96 ppm (aromatic protons), 3.65 ppm (-OCH$_2$CH$_2$O-), and 4.52ppm (-COOCCHO-). These results agree with the observation made by Qi and coworkers, who found similar signals in ^{1}H-NMR analysis of PEGDA.[21] The structure of aminated MNs is characterized by using XRD spectroscopy (Figure 2). Aminated MNs exhibit XRD peaks at 2θ of 30.3°, 35.7°, 43.4°, 54.2°, 57.3°, and 62.9° for the planes (311), (400), (422), (511), and (440), respectively (JCPDS card no. 19–0629). This suggests that functionalized magnetic nanoparticles are successfully produced.[22]

FTIR spectroscopy is used to confirm the functionalities present in PEG, PEGDA, aminated MNs, PEGDA-MN, PEGDA-MN-DOX, and DOX (Figure 3) at wavelengths ranging from 400 to 4000 cm^{-1}. The highest intensity of PEG bands is attributed to O-H stretching of the hydroxyl group at 3400 cm^{-1}, C-H stretching of alkanes at 2895 cm^{-1}, C-H scissor and bending at 1450–1292 cm^{-1}, C-O stretching of alcohol at 1245 cm^{-1}, and C-O-C stretching of ether at 1100–1060 cm^{-1}.[23] The structure of PEGDA is confirmed by the presence of a prominent band of aldehyde at 1725cm^{-1}. As indicated, the wide peak at 3450cm^{-1}, which corresponds to -OH stretching frequency, is less intensive. This reveals that PEG reacts with 4-carboxy benzaldehyde. MNs exhibit prominent bands at 578.97 and 623.11 cm^{-1}. This results from the Fe-O bond that is split from the bulk magnetite band at 570 cm^{-1}. These findings are most likely due to the tiny size of the MNs. The bands at 1622.97 and 3426.89 cm^{-1} correspond to NH_2 bending of the free NH_2 group and N-H stretching vibration, respectively. The amino group on the particle surface is made up of ethylene diamine molecules, which are used to make amino-MNs and are expected to be absorbed by the MNs surface. Similar bands have been observed by Unsoy and coworkers.[24] DOX bands are observed at 2929 (C-H), 1720 (C=O), 1621 and 1572

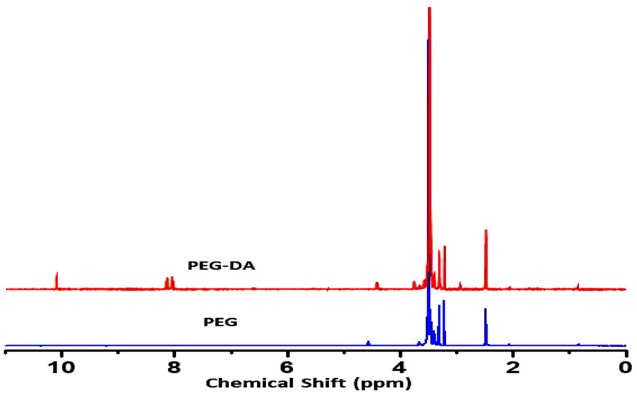

Figure 1 ^{1}H-NMR spectrum of pure PEG and PEG dialdehyde (PEG-DA).

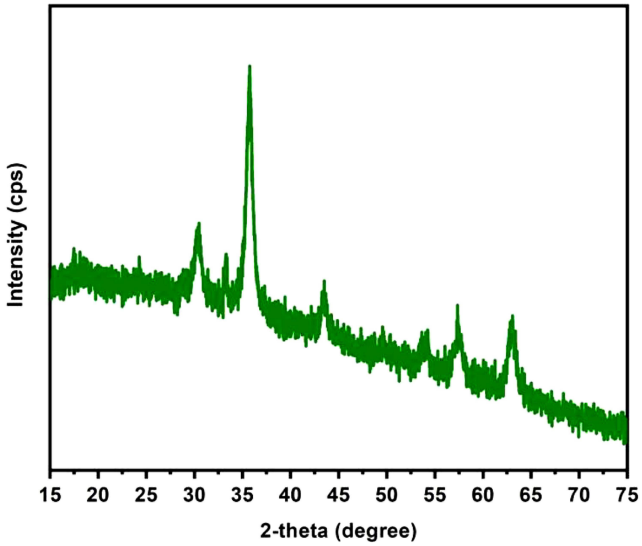

Figure 2 XRD patterns of aminated magnetic nanoparticles.

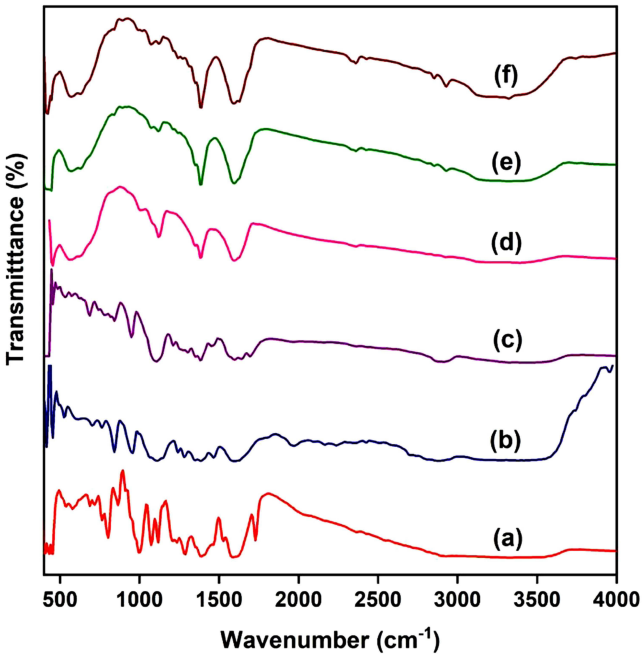

Figure 3 FTIR spectra of (**A**) DOX, (**B**) PEG, (**C**) PEGDA, (**D**) MNs, (**E**) PEGDA-MN and (**F**) PEGDA-MN-DOX.

(N-H), 1410 (C-C), and 1064 (C-O) cm^{-1}. These peaks are also present in the spectrum of PEGDA-MN-DOX, but have shifted to 2919 (C-H), 1718 (C=O), 1612 and 1570 (N-H), 1404 (C-C) and 1042 (C-O) cm^{-1}, respectively.[25] In the spectrum of the imine derivative, the aldehyde and amine signals disappear; however, signals for the -C-H, C=N, and Fe stretching are observed at 975.7 cm^{-1}, 1649cm^{-1} and 630 cm^{-1}, respectively. This indicates that the nanoparticles have successfully conjugated with functionalized MNs. This confirms the formation of PEGDA-MN. In the spectra of PEGDA-MN and PEGDA-MN-DOX, a new peak at 1346 cm^{-1} is found. This peak is assigned to the C-O-C asymmetric stretching vibrations of DOX. Another new peak is found at 2970 cm^{-1}. It results from the aromatic C-C stretching vibrations of DOX. The presence of it evidences that DOX is conjugated successfully into PEGDA-MN.[26]

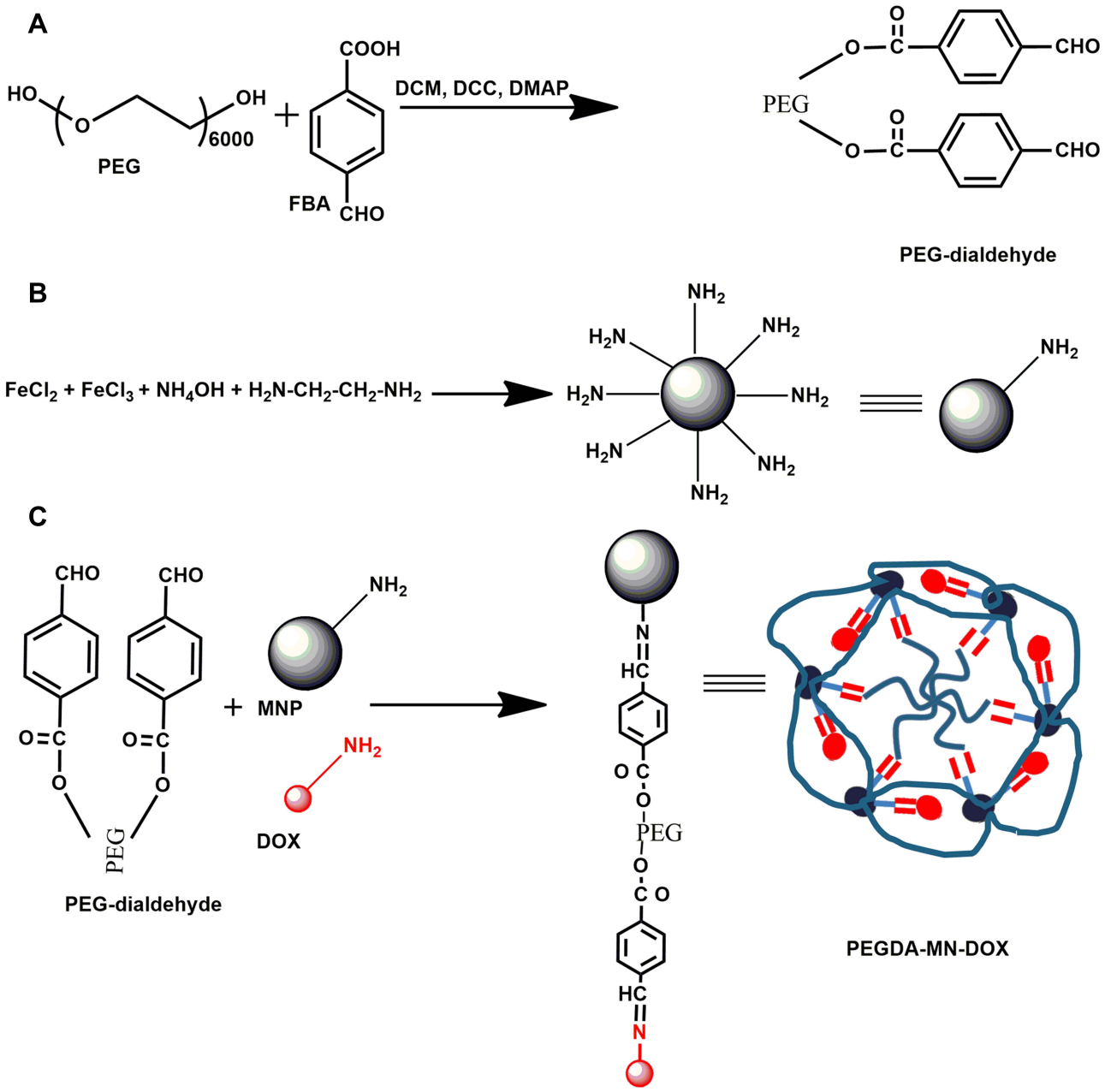

Scheme 1 Plausible route of synthesis of PEG-dialdehyde (**A**), aminated magnetic nanoparticles (**B**) and PEGDA-MN-DOX (**C**) (PEGDA-MN-DOX).

Overall, based on the ^{1}H NMR and FTIR results, the plausible route of synthesis of PEGDA-MN-DOX is shown in Scheme 1.

SEM, TEM and DLS Studies

The morphology of MN nanocomposites examined by SEM indicates that in the dry state of PEG-MN-DOX, magnetic nanoparticles are agglomerated due to the hydrophilicity of PEG chains (Figure 4). In addition, TEM characterization of PEG-MN-DOX reveals that the nanoparticles are formed in the core-shell structure manner with the size being around 20–50 nm (Figure 5). These results are further supported by the results of DLS analysis, in which the mean particle size

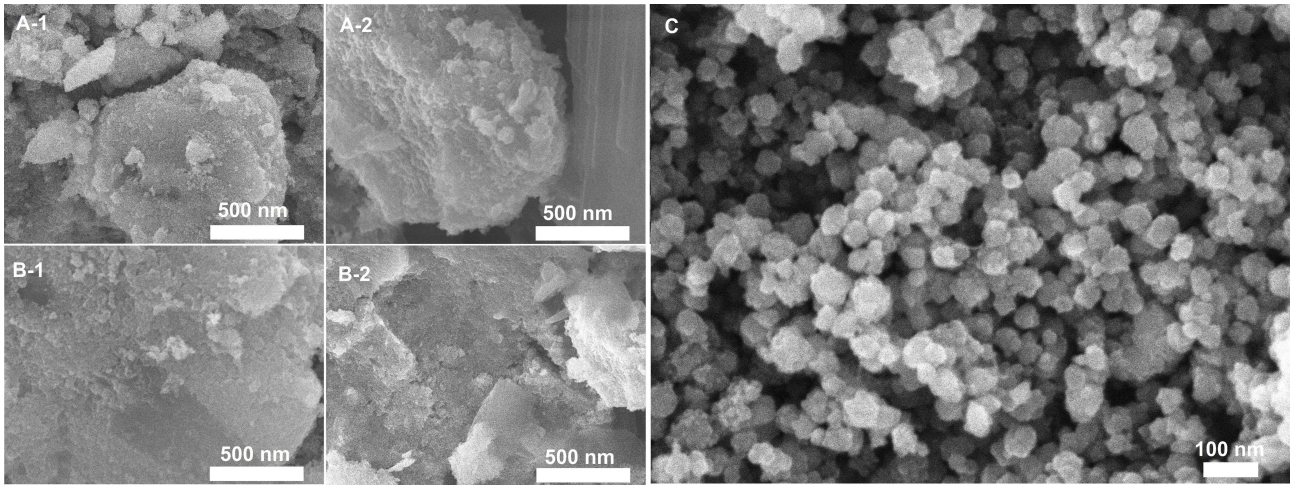

Figure 4 SEM images of PEG-coated aminated MN (**A**-1 and **A**-2), DOX-loaded PEGDA-aminated MNs. (**B**-1 and **B**-2) and magnetic nanoparticles (**C**).

of MNs is estimated to be 21.04nm with the polydispersity index being around 0.812. The mean particle size of PEG-MN-DOX magnetic nanoparticles is estimated to be 116.07nm with the polydispersity index being around 0.891.

TGA and DSC Studies

The TGA curve of PEGDA-MNs reveals a weight loss in the temperature range of 40 to 600°C (Figure 6A). This is related to the loss of adsorbed moisture. The thermogravimetric curve of doxorubicin similarly shows a three-stage weight loss pattern. The first stage occurs at temperatures ranging from 40 to 196°C, resulting in a 1.4% weight loss owing to evaporation of adsorbed moisture. The second and third phases occur at temperatures ranging from 198 to 261°C and 267 to 600°C, resulting in weight losses of 26 and 21%, correspondingly, and due to DOX degradation. In the TGA curves of PEGDA-MN, three weight loss peaks were observed, the first weight loss peak was observed at 98.6 to 91.99 weight % with a weight loss of 6.61 weight %, the second weight loss peak was observed with 6.54%, and the third weight loss peak was observed with 3.81 weight %. In PEGDA-MN-DOX, a two-stage weight loss was observed. The first weight loss peak was observed with weight % of 12.26 and the second weight loss peak was observed with an 8.83 weight loss percentage, PEGDA-MN-DOX is more thermally stable. This is attributed to the interactions between aminated iron oxide nanoparticles and polyethylene glycol. The DSC of pure DOX showed a peak at 247°C, corresponding to the melting endotherm of drugs. This peak was not identified in the drug-loaded PEG conjugate, suggesting that the DOX was chemically conjugated with PEGDA (Figure 6B).

Drug Conjugation and Release Studies

The conjugation of DOX to PEGDA along with MNs is estimated to be 48.6%. The release pattern of PEGDA-MN-DOX is examined at pH 1.2 and 7.4 at 37°C and 25°C (Figure 7). At pH 7.4, at the temperature of 37°C, 36%, 51%, 68% and 76% and at the temperature of 25°C 33%, 52%, 64% and 74% of the DOX is released after 24 h, 48 h, 72 h and 96 h. At the same time, at pH 1.2, at temperature 37°C, 31%, 46%, 63% and 71% and at temperature 25°C, 29%, 42%, 59% and 68% of the DOX is released after 24 h, 48 h, 72 h and 96 h.

To understand the release kinetics, four kinetic models are presented below. The zero-order kinetic model is named after the fact that the rate of drug release is unchanged by its concentration.[27] The expression, according to the model.

$$Q_t = Q_0 - K_0 t$$

The drug release is defined by (K_0 is the zero-order rate constant and t is the time). If this model is accurate, a plot of the quantity of drug released vs time will be linear, and the drug release will be perfect, with the same quantity of medication

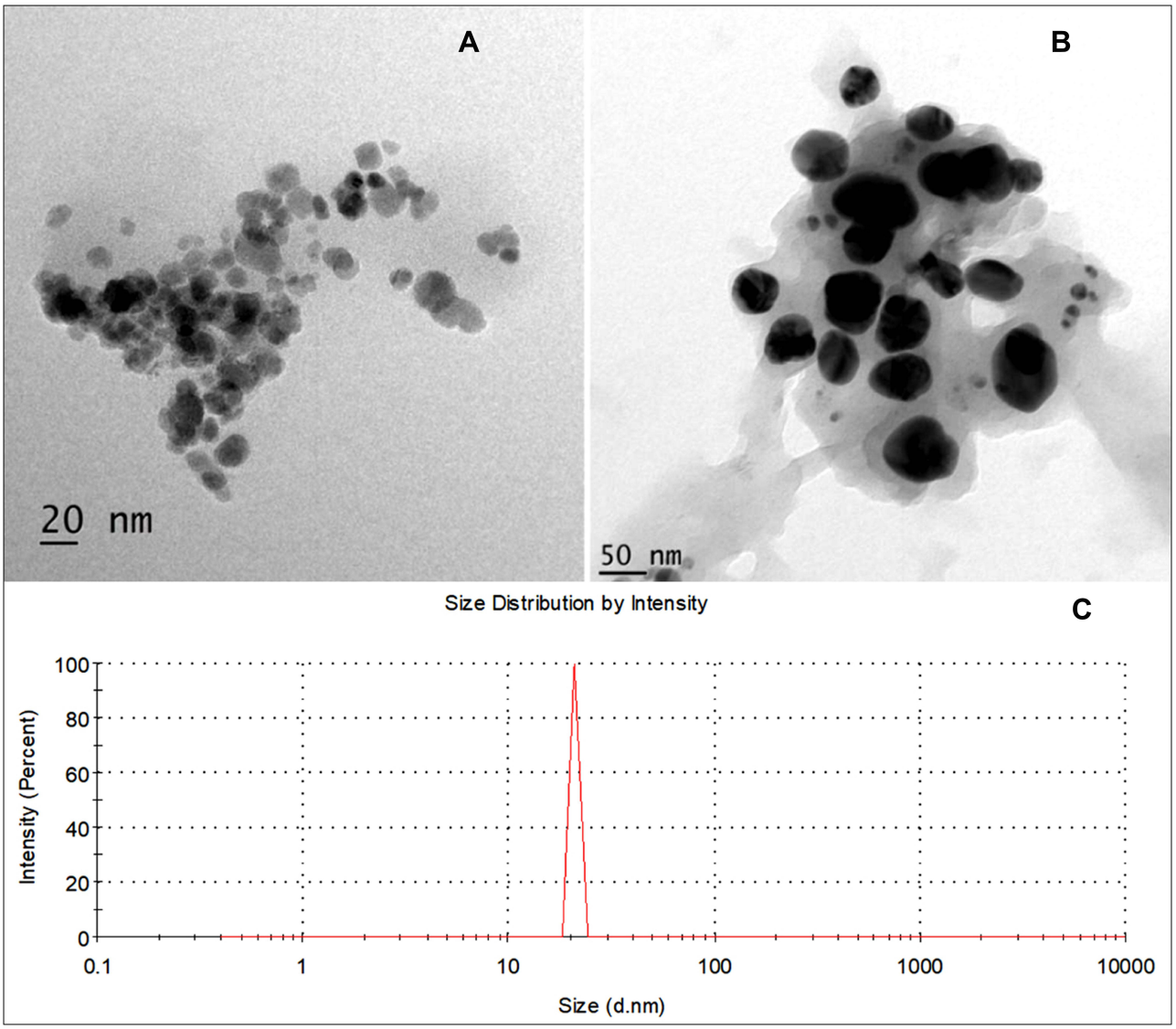

Figure 5 TEM images of PEGDA-MN-DOX with different magnification (**A** and **B**) and the corresponding DLS diagram (**C**).

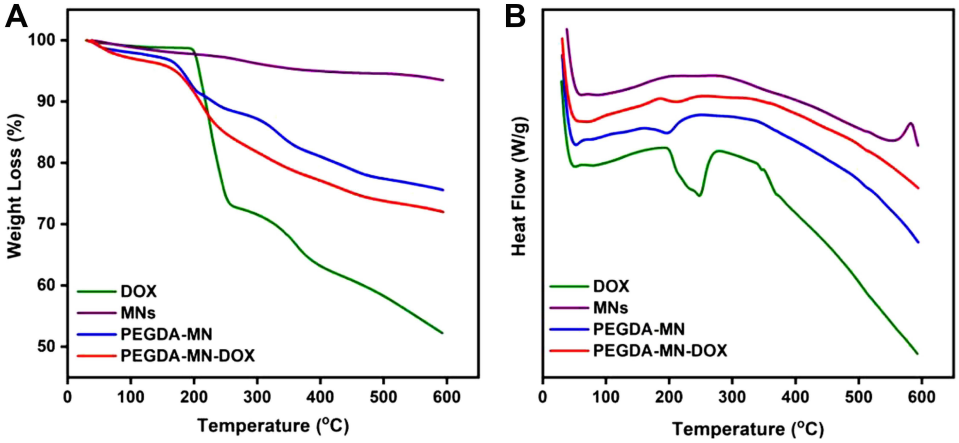

Figure 6 (**A**) TGA and (**B**) DSC graphs of DOX, AMNs, PEGDA-MN, and PEGDA-MN-DOX nanoparticles.

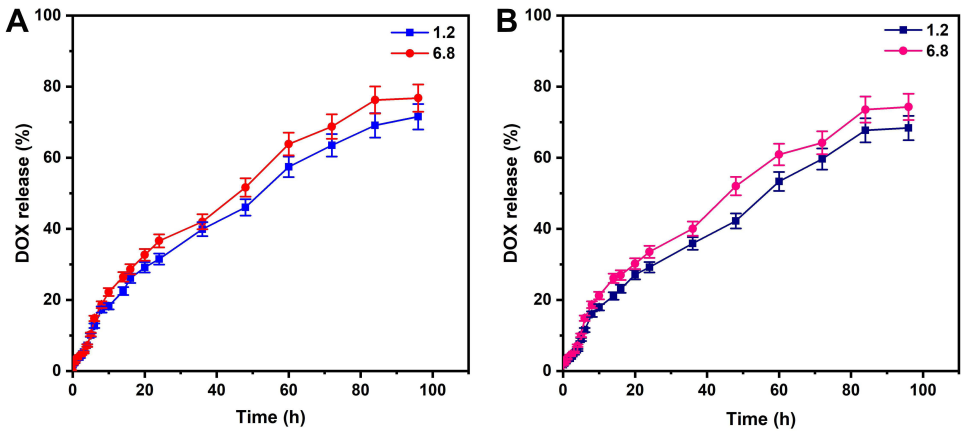

Figure 7 Drug release studies of DOX from PEGDA-MN-DOX at (**A**) 37°C and (**B**) 25°C.

released every t seconds. The drug release rate is proportional to the drug concentration on the polymer matrix, according to the first-order rate equation. The following formula describes the model:

$$lnQ_t = lnQ_0 - K_1$$

(The amount of medication not released in time t is Q_t, Q_0, and the first-order constant is K_1.)

First-order drug release kinetics are predicted by the linear relationship between the log of cumulative percent drug unreleased and t. The equation represents the Higuchi model.

$$Q_t = K_h t^{1/2}$$

The Higuchi model drug release may be correlated to the linear relationship between Q_t and $t_{1/2}$ above equation. The dissolution rate is controlled via a diffusion mechanism based on Fick's law, according to the Higuchi model.

The experimental equation is provided by Korsmeyer and Peppas to characterize both Fickian and non-Fickian drug release from swelling as well as non-swelling polymeric delivery devices. The Korsmeyer and Peppas model has the following mathematical equation.

$$\frac{M_t}{M_\infty} = Kt^n$$

$\frac{M_t}{M_\infty}$ is the percentage of drug released at time t, n denotes the drug's transport pathway, and K denotes the kinetic constant.[28] For the n value of the Korsmeyer–Peppas models, $n \leq 0.45$ correlates for Fickian diffusion release and $0.45 < n < 0.89$ for non-Fickian release (anomalous). The quasi Fickian and Fickian release correspond to the non-

Table 1 Release Kinetic Parameters of PEGDA-MN-DOX. Nanoparticles at Different pH Values (7.4 and 1.2) and Temperatures (37°C and 25°C)

pH	Temperature (°C)	Zero-Order Model		First-Order Model		Higuchi Model		Korsmeyer-Peppas Model	
		K_0	r^2	K_1	r^2	K_H	r^2	n	r^2
1.2	37	0.887	0.8942	0.015	0.9803	6.959	0.9694	0.731	0.9838
	25	0.839	0.9116	0.013	0.9793	6.544	0.9613	0.739	0.9801
7.4	37	0.972	0.8784	0.017	0.9806	7.647	0.9698	0.758	0.9803
	25	0.933	0.8797	0.016	0.9778	7.339	0.9710	0.714	0.9732

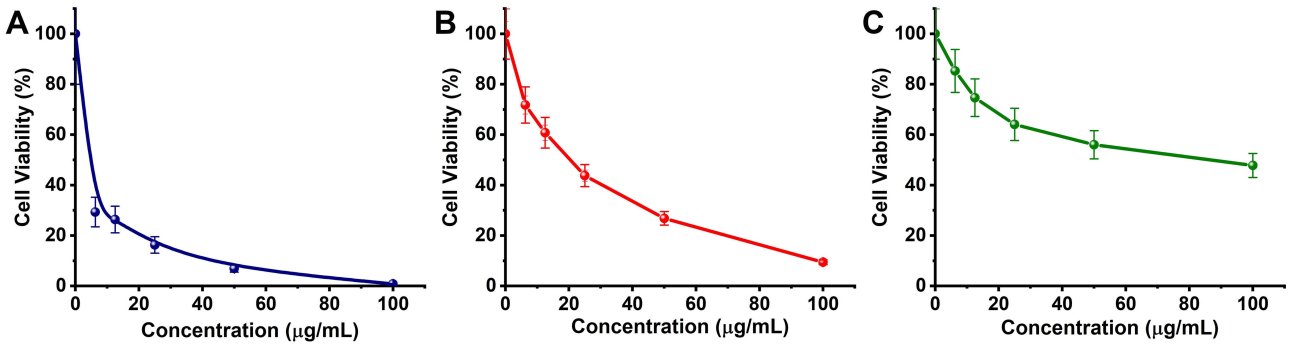

Figure 8 Cell viability of MCF-7 cell line against (**A**) DOX, (**B**) PEGDA-MN, and (**C**) PEGDA-MN-DOX nanoparticles.

swellable matrix diffusion and non-Fickian release (anomalous) correlates to both diffusion and relaxation mechanisms.

The r^2 values found after fitting the release data into various kinetic models are shown in Table 1. The PEGDA-MN-DOXrelease profiles suit both the first-order model and the Higuchi model. The drug release process, therefore, involves the uptake of PBS into the polymer matrix and the diffusion of DOX molecules from the nano composites to the external release medium, with the release rate being directly proportional to the drug concentration. Furthermore, 60% of the release data is fitted into the Korsmeyer-Peppas equation to establish the release mechanism of PEGDA-MN-DOX nanoparticles. The *n* values vary from 0.714 to 0.758, demonstrating that PEGDA-MN-DOX diffuses via a non-Fickian route.

Cytotoxic and ROS Studies

MCF-7 cells were used to find the anticancer potential of DOX, PEGDA-MN, and PEGDA-MN-DOX nanoparticles (Figure 8). The MTT results showed that both PEGDA-MN and PEGDA-MN-DOX nanoparticles could kill cancer cells. The number of MCF-7 cells still alive after exposure to PEGDA-MN, and PEGDA-MN-DOX nanoparticles were 47 and 9.4%, respectively, suggesting that the viability of conjugates is lower than that of DOX. This is because the drug from the drug conjugates is sustained release. This statement fits with previous research,[29–31] which found that a drug's toxicity is lower when it is released slowly over time. Interestingly, PEGDA-MN nanoparticles showed toxic effects even though they do not contain drug substances, demonstrating that the developed conjugates had an anticancer impact, at least partially facilitated by the production of reactive oxygen species. This argument is evidenced by the fact that treatment with conjugates causes a rise in the ROS level found within the MCF-7 cells (Figure 9A). These results are

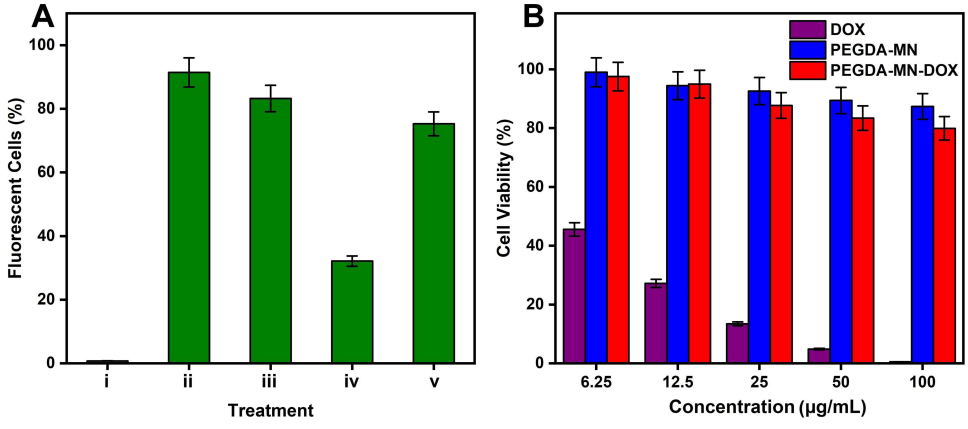

Figure 9 (**A**) The H_2DCFDA assay can be used to measure the ROS activity inside MCF-7 cells after they have been treated with various substances: (i) no treatment, (ii) treatment with H_2O_2, (iii) treatment with DOX, (iv) treatment with PEGDA-MNs, and (v) treatment PEGDA-MN-DOX. (**B**) Cell viability of 3T3 cell line against DOX, PEGDA-MN, and PEGDA-MN-DOX nanoparticles.

supported by Reddy and Lai,[31] who found a ROS effect in their nanocomposites embedded with magnetic nanoparticles. In addition to MCF-7 cells, 3T3 fibroblast cells are also utilized to evaluate the biocompatibility of drug conjugates. After 24 h of treatment with drug-conjugate and AMNs at various concentrations, more than 80% of the cells are still alive (Figure 9B). This shows that the toxicity of drug conjugates depends on the type of cell since they are more toxic to MCF-7 cells but not harmful to 3T3 cells.

Conclusion

Effective carriers enable effective drug encapsulation and sustained drug release. Over the years, different carriers have been developed, but the therapeutic action elicited by those carriers is dependent solely on the therapeutic effect of the loaded drug. We hypothesize that the therapeutic effect of the treatment would be enhanced if the carrier itself could also play an active role in combating cancer. To achieve this, we have generated in this study a highly versatile and multifunctional drug conjugates, PEGDA-MN-DOX, which not only shows high drug encapsulation efficiency and high drug release sustainability but also displays intrinsic cancer-targeting capacity and ROS-generating ability. The latter unique properties significantly enhance the effect of the carriers in killing cancer cells. Regarding the encouraging in vitro performance of our carrier, it is anticipated that the reported drug delivery system has been confirmed to show anticancer potential, cancer-targeting ability, and ROS-generating capacity for effective drug encapsulation and sustained release in chemotherapy.

Disclosure

The authors report no conflicts of interest in this work.

References

1. Messersmith PB, Giannelis EP. Synthesis and barrier properties of poly(ε-caprolactone)-layered silicate nanocomposites. *J Polym Sci Pol Chem*. 1995;33(7):1047–1057. doi:10.1002/pola.1995.080330707
2. Sylla BS, Wild CP. A million Africans a year dying from cancer by 2030: what can cancer research and control offer to the continent? *Int J Cancer*. 2012;130(2):245–250. doi:10.1002/ijc.26333
3. Soares PIP, Sousa AI, Silva JC, Ferreira IMM, Novo CMM, Borges JP. Chitosan-based nanoparticles as drug delivery systems for doxorubicin: optimization and modelling. *Carbohydr Polym*. 2016;147:304–312. doi:10.1016/j.carbpol.2016.03.028
4. Panyam J, Labhasetwar V. Dynamics of endocytosis and exocytosis of poly(D,L-Lactide-co-Glycolide) nanoparticles in vascular smooth muscle cells. *Pharm Res*. 2003;20(2):212–220. doi:10.1023/A:
5. Bahadar H, Maqbool F, Niaz K, Abdollahi M. Toxicity of nanoparticles and an overview of current experimental models. *Iran Biomed J*. 2016;20 (1):1–11. doi:10.7508/ibj.2016.01.001
6. Seenuvasan M, Vinodhini G, Malar CG, Balaji N, Kumar KS. Magnetic nanoparticles: a versatile carrier for enzymes in bio-processing sectors. *IET Nanobiotechnol*. 2018;12(5):535–548. doi:10.1049/iet-nbt.2017.0041
7. Dabbagh A, Abdullah BJJ, Abdullah H, Hamdi M, Kasim NHA. Triggering mechanisms of thermosensitive nanoparticles under hyperthermia condition. *J Pharm Sci*. 2015;104(8):2414–2428. doi:10.1002/jps.24536
8. Takae S, Miyata K, Oba M, et al. PEG-detachable polyplex micelles based on disulfide-linked block catiomers as bioresponsive nonviral gene vectors. *J Am Chem*. 2008;130(18):6001–6009. doi:10.1021/ja800336v
9. Teicher BA. Molecular targets and cancer therapeutics: discovery, development and clinical validation. *Drug Resist Updat*. 2000;3(2):67–73. doi:10.1054/drup.2000.0123
10. Yoo HS, Lee KH, Oh JE, Park TG. In vitro and in vivo anti-tumor activities of nanoparticles based on doxorubicin–PLGA conjugates. *J Control Release*. 2000;68(3):419–431. doi:10.1016/S0168-3659(00)00280-7
11. Behl A, Parmar VS, Malhotra S, Chhillar AK. Biodegradable diblock copolymeric PEG-PCL nanoparticles: synthesis, characterization and applications as anticancer drug delivery agents. *Polymer*. 2020;207:122901. doi:10.1016/j.polymer.2020.122901
12. Rao KS, Chung I, Reddy KM, Ha C-S. PMMA-based microgels for controlled release of an anticancer drug. *J Appl Polym Sci*. 2009;111 (2):845–853. doi:10.1002/app.29057
13. Madhusudana Rao K, Krishna Rao KSV, Ramanjaneyulu G, Ha C-S. Curcumin encapsulated pH sensitive gelatin based interpenetrating polymeric network nanogels for anti cancer drug delivery. *Int J Pharm*. 2015;478(2):788–795. doi:10.1016/j.ijpharm.2014.12.001
14. Reddy PRS, Rao KS, Rao KM, Reddy NS, Eswaramma S. pH sensitive poly(methyl methacrylate-co-acryloyl phenylalanine) nanogels and their silver nanocomposites for biomedical applications. *J Drug Deliv Sci Technol*. 2015;29:181–188. doi:10.1016/j.jddst.2015.07.002
15. Krishna Rao KSV, Ramasubba Reddy P, Lee Y-I, Kim C. Synthesis and characterization of chitosan–PEG–Ag nanocomposites for antimicrobial application. *Carbohydr Polym*. 2012;87(1):920–925. doi:10.1016/j.carbpol.2011.07.028
16. Rao KS, Subha MCS, Sairam M, Halligudi SB, Aminabhavi TM. Synthesis, characterization and controlled release characteristics of PEGylated hydrogels for diclofenac sodium. *Des Monomers Polym*. 2006;9(3):261–273. doi:10.1163/156855506777350992
17. Rao KS, Zhong Q, Bielski ER, da Rocha SRP. Nanoparticles of pH-Responsive, PEG–doxorubicin conjugates: interaction with an in vitro model of lung adenocarcinoma and their direct formulation in propellant-based portable inhalers. *Mol Pharm*. 2017;14(11):3866–3878. doi:10.1021/acs.molpharmaceut.7b00584

18. Akbarzadeh A, Mikaeili H, Zarghami N, Mohammad R, Barkhordari A, Davaran S. Preparation and in vitro evaluation of doxorubicin-loaded Fe_3O_4 magnetic nanoparticles modified with biocompatible copolymers. *Int J Nanomedicine*. 2012;7:511–526. doi:10.2147/IJN.S24326
19. Jahangiri S, Akbarzadeh A. RETRACTED ARTICLE: preparation and in vitro evaluation of Methotrexate-loaded magnetic nanoparticles modified with biocompatible copolymers. *Artif Cells Nanomed Biotechnol*. 2016;44(7):1733–1740. doi:10.3109/21691401.2015.1090443
20. Obireddy SR, Lai WF. Multi-component hydrogel beads incorporated with reduced graphene oxide for pH-responsive and controlled co-delivery of multiple agents. *Pharmaceutics*. 2021;13(3):313. doi:10.3390/pharmaceutics13030313
21. Qi P, Wu X, Liu L, Yu H, Song S. Hydrazone-containing triblock copolymeric micelles for pH-controlled drug delivery. *Front Pharmacol*. 2018;9:12. doi:10.3389/fphar.2018.00012
22. Songvorawit N, Tuitemwong K, Tuitemwong P. Single step synthesis of amino-functionalized magnetic nanoparticles with polyol technique at low temperature. *ISRN Nanotechnology*. 2011;2011:483129. doi:10.5402/2011/483129
23. Pramono E, Utomo SB, Wulandari V, Zahrotul WA, Clegg F, Clegg F. FTIR studies on the effect of concentration of polyethylene glycol on polimerization of Shellac. *J Phys Conf Ser*. 2016;776:012053. doi:10.1088/1742-6596/776/1/012053
24. Unsoy G, Khodadust R, Yalcin S, Mutlu P, Gunduz U. Synthesis of Doxorubicin loaded magnetic chitosan nanoparticles for pH responsive targeted drug delivery. *Eur J Pharm Sci*. 2014;62:243–250. doi:10.1016/j.ejps.2014.05.021
25. Mauri E, Rossi F, Sacchetti A. Simple and efficient strategy to synthesize PEG-aldehyde derivatives for hydrazone orthogonal chemistry. *Polym Adv Technol*. 2015;26(12):1456–1460. doi:10.1002/pat.3578
26. Antarnusa G, Suharyadi E. A synthesis of polyethylene glycol (PEG)-coated magnetite Fe_3O_4 nanoparticles and their characteristics for enhancement of biosensor. *Mater Res Express*. 2020;7(5):056103. doi:10.1088/2053-1591/ab8bef
27. Kalam MA, Humayun M, Parvez N, et al. Release kinetics of modified pharmaceutical dosage forms: a review. *Cont J Pharm Sci*. 2007;1(1):30–35.
28. Korsmeyer RW, Peppas NA. Solute and penetrant diffusion in swellable polymers. III. Drug release from glassy poly(HEMA-co-NVP) copolymers. *J Control Release*. 1984;1(2):89–98. doi:10.1016/0168-3659(84
29. Boddu A, Obireddy SR, Subbarao SMC, Rao KM, Venkata KR. Encapsulation of 5-fluorouracil treated reduced graphene oxide in sodium alginate matrix for controlled and pH-responsive drug delivery. *ChemistrySelect*. 2021;6(25):6533–6540. doi:10.1002/slct.202101395
30. Lai W-F, Huang EM, Wong W-T. A gel-forming clusteroluminogenic polymer with tunable emission behavior as a sustained-release carrier enabling real-time tracking during bioactive agent delivery. *Appl Mater Today*. 2020;21:100876. doi:10.1016/j.apmt.2020.100876
31. Obireddy SR, Lai WF. ROS-generating amine-functionalized magnetic nanoparticles coupled with carboxymethyl chitosan for pH-responsive release of doxorubicin. *Int J Nanomed*. 2022;17:589–601. doi:10.2147/IJN.S338897